Available online at www.sciencedirect.com
ScienceDirect
International Journal of Heat and Mass Transfer 51 (2008) 3460–3467
International Journal of HEAT and MASS TRANSFER
www.elsevier.com/locate/ijhmt

Laminar forced convection slip-flow in a micro-annulus between two concentric cylinders

Mete Avcı, Orhan Aydın *

Karadeniz Technical University, Department of Mechanical Engineering, 61080 Trabzon, Turkey

Received 13 September 2006
Available online 22 January 2008

Abstract

Forced convection heat transfer in hydrodynamically and thermally fully developed flows of viscous dissipating gases in annular microducts between two concentric micro cylinders is analyzed analytically. The viscous dissipation effect, the velocity slip and the temperature jump at the wall are taken into consideration. Two different cases of the thermal boundary conditions are considered: uniform heat flux at the outer wall and adiabatic inner wall (Case A) and uniform heat flux at the inner wall and adiabatic outer wall (Case B). Solutions for the velocity and temperature distributions and the Nusselt number are obtained for different values of the aspect ratio, the Knudsen number and the Brinkman number. The analytical results obtained are compared with those available in the literature and an excellent agreement is observed.

Keywords: Microscale; Concentric annular duct; Knudsen number; Heat transfer; Slip-flow; Temperature jump; Viscous dissipation

1. Introduction

Fluid flow and heat transfer at microscale have attracted an important research interest in recent years due to the rapid growth of novel techniques applied in MEMS (microelectromechanical systems) and biomedical applications such as drug delivery, DNA sequencing, and bio-MEMS. Readers are referred to see recent excellent reviews related to transport phenomena in microchannels by Ho and Tai [1], Palm [2], Sobhan and Garimella [3], Obot [4] Rostami et al. [5,6], Gad-el-Hak [7], Guo and Li [8,9], Morini [10].

It is experimentally shown that fluid flow and heat transfer at microscale differ greatly from those at macroscale, especially in terms of wall friction and heat transfer performance, with generally inconsistent and contradictory experimental results published. Therefore, there is a need and a good potential for theoretical investigations. At macroscale, classical conservation equations are successfully coupled with the corresponding wall boundary conditions, usual no-slip for the hydrodynamic boundary condition and no-temperature-jump for the thermal boundary condition. These two boundary conditions are valid only if the fluid flow adjacent to the surface is in thermal equilibrium. However, they are not valid for gas flow at microscale. For this case, the gas no longer reaches the velocity or the temperature of the surface and therefore a slip condition for the velocity and a jump condition for the temperature should be adopted.

Barron et al. [11,12] extended the Graetz problem to slip-flow and developed simplified relationships to describe the effect of slip-flow on the convection heat transfer coefficient. Ameel et al. [13] analytically treated the problem of laminar gas flow in microtubes with a constant heat flux boundary condition at the wall assuming a slip-flow hydrodynamic condition and a temperature jump thermal condition at the wall. They disclosed that the fully developed Nusselt number decreased with Knudsen number. In recent

* Corresponding author. Tel.: +90 (462) 377 29 74; fax: +90 (462) 325 55 26.
E-mail address: oaydin@ktu.edu.tr (O. Aydın).

0017-9310/$ - see front matter © 2007 Elsevier Ltd. All rights reserved.
doi:10.1016/j.ijheatmasstransfer.2007.10.036

Nomenclature

A	cross-sectional area (m^2)
Br	Brinkman number, Eq. (15)
c_p	specific heat at constant pressure (k J/kg K)
D_h	hydraulic diameter of the annuli $= 2(r_o - r_i)$ (m)
F	tangential momentum accommodation coefficient
F_t	thermal accommodation coefficient
h	convective heat transfer coefficient (W/m^2 K)
k	thermal conductivity (W/m K)
Kn	Knudsen number $= \lambda/D_h$
Nu	Nusselt number $= hD_h/k$
Pr	Prandtl number $= \mu c_p/k$
q_w	wall heat flux (W/m^2)
r	radial coordinate (m)
r^*	aspect ratio for the annuli $= r_i/r_o$
r_i	inner radius of the annuli (m)
r_m	the radius where the maximum velocity occurs (m)
r_m^*	dimensionless form of r_m, Eq. (9)
r_o	outer radius of the annuli
R	dimensionless radial coordinate $= r/r_o$
T	temperature (K)
u	velocity (m/s)
U	dimensionless velocity $= u/u_m$
z	axial direction (m)

Greek symbols

α	thermal diffusivity (m^2/s)
λ	molecular mean free path
γ	specific heat ratio
μ	dynamic viscosity (Pa s)
ρ	density (kg/m^3)
ν	kinematic viscosity (m^2/s)
θ	dimensionless temperature, Eq. (13)

Subscripts

m	mean
s	fluid properties at the wall
w	wall

studies, Aydın and Avcı [14–17] theoretically investigated the steady, laminar forced convective heat transfer of a Newtonian fluid in a microtube and microduct between two parallel plates including the velocity slip and the temperature jump at the wall for the fully developed flow case [14,15] and for the thermally developing flow [16,17].

An example of micro heat exchangers is the one for which the hot and cold fluids move in the same or opposite directions in a concentric microtube. Fabrication of such microexchangers is now possible due to recent innovative microfabrication techniques such as etching/lithography/deposition and silicon micromachining. Such a geometry can also be found in cooling of high power resistive magnets, compact fission reactor cores, fusion reactor blankets, advanced space thermal management systems, manufacturing and material processing operations and high-density multi-chip modules in supercomputers and other modular electronics [18]. The objective of the present study is to theoretically investigate the gas flow in a concentric annular microduct representing a micro heat exchanger for the hydrodynamically and thermally fully developed case. The effect of the Knudsen number, the aspect ratio of the annular geometry and the Brinkman number on the temperature profile and, in the following, the Nusselt number are determined for two different configurations of the thermal boundary conditions.

2. Analysis

Consider hydrodynamically and thermally fully developed, steady, laminar flow having constant properties (i.e. the thermal conductivity and the thermal diffusivity of the fluid are considered to be independent of temperature). The viscous dissipation effect of the fluid is included. The axial heat conduction in the fluid and in the wall is assumed to be negligible.

In this study, the usual continuum approach is coupled with the two main characteristics of the microscale phenomena, the velocity slip and the temperature jump. Velocity slip is defined as [13]

$$u_s = -\frac{2-F}{F}\lambda\left.\frac{\partial u}{\partial r}\right|_{r=r_0} \tag{1}$$

where u_s is the slip velocity, λ is the molecular mean free path, and F is the tangential momentum accommodation coefficient, and the temperature jump is defined as [13]

$$T_s - T_w = -\frac{2-F_t}{F_t}\frac{2\gamma}{\gamma+1}\frac{\lambda}{Pr}\left.\frac{\partial T}{\partial r}\right|_{r=r_0} \tag{2}$$

where T_s is the temperature of the gas at the wall, T_w is the wall temperature, and F_t is the thermal accommodation coefficient. F and F_t are parameters that describe gas–surface interaction and are functions of the composition and temperature of gas, the gas velocity over the surface, and the solid surface temperature, chemical state and roughness [13]. Particularly for air and for most engineering applications, they assume typical values near unity [13], which represents the diffuse reflection case [19]. For the rest of the analysis, F and F_t will be shown by F.

The momentum equation in the z-direction is described as

$$\frac{1}{r}\frac{\partial}{\partial r}\left(r\frac{\partial u}{\partial r}\right) = \frac{1}{\mu}\frac{dP}{dz} = \text{const} \tag{3}$$

Setting $F = 1$ in Eq. (1) will lead to the following boundary conditions:

$$\begin{aligned} r &= r_i \quad u = u_s = \lambda\left(\frac{\partial u}{\partial r}\right)_{r=r_i} \\ r &= r_o \quad u = u_s = -\lambda\left(\frac{\partial u}{\partial r}\right)_{r=r_o} \end{aligned} \tag{4}$$

and using the following dimensionless parameters:

$$R = \frac{r}{r_o} \quad r^* = \frac{r_i}{r_o} \quad U = \frac{u}{u_m} \tag{5}$$

Eq. (3) is solved to give the dimensionless velocity distributions as

$$U = 2(1 - R^2 + 2r_m^{*2}\ln(R) + A)/B \tag{6}$$

where A and B are, respectively

$$A = 4Kn(1 - r^*)(1 - r_m^{*2}) \tag{7}$$

$$B = \left(1 - r^{*2} - 4r_m^{*2}\left(\frac{1}{2} + \frac{r^{*2}}{1 - r^{*2}}\ln(r^*)\right) + 8Kn(1 - r^*)(1 - r_m^{*2})\right) \tag{8}$$

Here Kn is Knudsen number ($Kn = \lambda/D_h$) and r_m^* designates the dimensionless radius where the maximum velocity occurs ($\partial u/\partial r = 0$). It is given by

$$r_m^* = \frac{r_m}{r_o} = \left(\frac{(1 - r^{*^2})(1 + 4Kn)}{2\ln(1/r^*) - 4Kn\left(\frac{r^{*2}-1}{r^*}\right)}\right)^{1/2} \tag{9}$$

The conservation of energy including the effect of the viscous dissipation requires

$$u\frac{\partial T}{\partial z} = \frac{\alpha}{r}\frac{\partial}{\partial r}\left(r\frac{\partial T}{\partial r}\right) + \frac{v}{c_p}\left(\frac{\partial u}{\partial r}\right)^2 \tag{10}$$

where the second term in the right hand side is the viscous dissipation term.

The constant heat flux at wall is assumed at the wall, which states that

$$k\left.\frac{\partial T}{\partial r}\right|_{r=r_o} = q_w \tag{11}$$

where q_w is positive when its direction is to the fluid (from the hot wall), otherwise it is negative (to the cold wall).

For the uniform wall heat flux case, the first term in the left-side of Eq. (10) is

$$\frac{\partial T}{\partial z} = \frac{dT_w}{dz} = \frac{dT_s}{dz} \tag{12}$$

Introduction of the following non-dimensional temperature:

$$\theta = \frac{T - T_s}{\frac{q_w r_o}{k}} \tag{13}$$

modifies Eq. (10) into the following dimensionless form:

$$\frac{1}{R}\frac{d}{dR}\left(R\frac{d\theta}{dR}\right) = aU - Br\left(\frac{dU}{dR}\right)^2 \tag{14}$$

where $a = \frac{u_m k r_o}{\alpha q_w}\frac{dT_s}{dz}$ and Br is the Brinkman number given as

$$Br = \frac{\mu u_m^2}{q_w r_o} \tag{15}$$

Two different forms of the thermal boundary conditions are applied, which are shown in Fig. 1. In the following, these two different cases are treated separately:

For the Case A, the thermal boundary conditions in the dimensionless form are written as

$$\begin{aligned} \theta &= 0 \quad \left.\frac{\partial\theta}{\partial R}\right|_{R=1} = 1 \text{ at } R = 1 \\ &\left.\frac{\partial\theta}{\partial R}\right|_{R=r^*} = 0 \text{ at } R = r^* \end{aligned} \tag{16}$$

The solution of a and Eq. (14) under the thermal boundary conditions given above in Eq. (16) are obtained as, respectively

$$a = \frac{-2B^2 + 8Br(r^{*2} - 1)(1 - 4r_m^{*2} + r^{*2}) + 32Brr_m^{*4}\ln(r^*)}{B((1 + 2A - 2r_m^{*2} - r^{*2})(r^{*2} - 1) + 4Br_m^{*2}r^{*2}\ln(r^*))} \tag{17}$$

$$\begin{aligned} \theta(R) = \frac{T - T_s}{q_w r_o/k} = \frac{a}{2B}(&-3 - A + 2r_m^{*2} + R^2(1 + A - 2r_m^{*2} + R^2/2) \\ &- \ln R(1 + 2A - 2r_m^{*2}(1 + \ln R))) + \frac{.Br}{B^2}((1 - R^2) \\ &\times (1 + R^2 - 8r_m^{*2}) + 4\ln R(1 - 4r_m^{*2}) - 8r_m^{*4}(\ln R)^2) + \ln R \end{aligned} \tag{18}$$

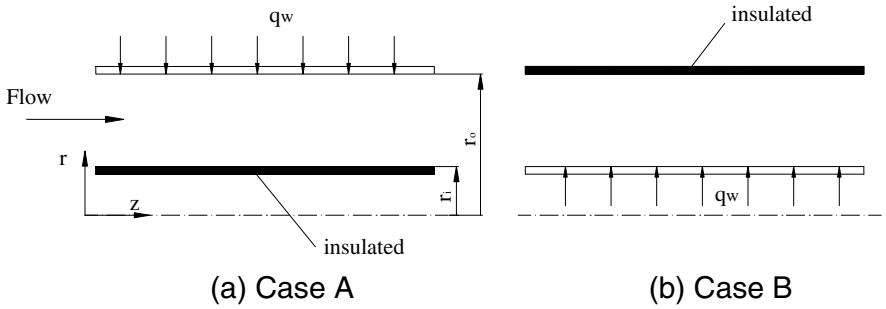

Fig. 1. Boundary conditions and schematic diagram of flow domain.

In the Case B, the dimensionless-type thermal boundary conditions are as in the following:

$$\theta = 0 \quad \left.\frac{\partial\theta}{\partial R}\right|_{R=r^*} = -1 \ \text{ at } R = r^* \qquad \left.\frac{\partial\theta}{\partial R}\right|_{R=0} = 0 \ \text{ at } R = 1 \tag{19}$$

Similarly, the solution of Eq. (14) under the conditions of Eq. (19) gives

$$a = \frac{-2B^2 r^* + 8Br(r^{*2}-1)(1-4r_m^{*2}+r^{*2}) + 32Brr_m^{*4}\ln(r^*)}{B((1+2A-2r_m^{*2}-r^{*2})(r^{*2}-1)+4r_m^{*2}r^{*2}\ln(r^*))} \tag{20}$$

$$\begin{aligned}\theta(R) = \frac{T-T_s}{q_w r_o/k} = \frac{a}{2B}&((R^2-r^{*2})(1+A-2r_m^{*2}) - (R^2-r^{*2}) \\ &- (\ln R - \ln r^*)(1+2A-2r_m^{*2}) + 2r_m^{*2}(R^2\ln R - r^{*2}\ln r^*)) \\ &+ \frac{.Br}{B^2}((R^2-r^{*2})(8r_m^{*2}-(R^2+r^{*2})) \\ &+ 4(\ln R - \ln r^*)(1-4r_m^{*2}) - 8r_m^{*4}((\ln R)^2 - (\ln r^*)^2))\end{aligned} \tag{21}$$

Eqs. (18) and (21) which are in terms of T_s (Note again T_s is the temperature of the fluid at the wall) can be transformed into the equations in terms of T_w, the wall temperature using the following conversion formula:

$$\frac{T_s - T_w}{q_w r_0/k} = -\frac{4\gamma}{\gamma+1}\frac{Kn}{\mathrm{Pr}}(1-r^*)$$

Then Eqs. (18) and (21) become, respectively,

$$\begin{aligned}\theta^*(R) &= \frac{T-T_s}{q_w r_o/k} + \frac{T_s - T_w}{q_w r_0/k} = \frac{T-T_w}{q_w r_0/k} \\ &= \frac{a}{2B}(-3-A+2r_m^{*2} + R^2(1+A-2r_m^{*2} \\ &\quad + R^2/2) - \ln R(1+2A-2r_m^{*2}(1+\ln R))) \\ &\quad + \frac{.Br}{B^2}((1-R^2)(1+R^2-8r_m^{*2}) + 4\ln R(1-4r_m^{*2}) \\ &\quad - 8r_m^{*4}(\ln R)^2) + \ln R - \frac{4\gamma}{\gamma+1}\frac{Kn}{\mathrm{Pr}}(1-r^*)\end{aligned} \tag{22}$$

and

$$\begin{aligned}\theta^*(R) = \frac{a}{2B}&((R^2-r^{*2})(1+A-2r_m^{*2}) - (R^2-r^{*2}) \\ &- (\ln R - \ln r^*)(1+2A-2r_m^{*2}) + 2r_m^{*2}(R^2\ln R \\ &- r^{*2}\ln r^*)) + \frac{.Br}{B^2}((R^2-r^{*2})(8r_m^{*2}-(R^2+r^{*2})) \\ &+ 4(\ln R - \ln r^*)(1-4r_m^{*2}) - 8r_m^{*4}((\ln R)^2 - (\ln r^*)^2)) \\ &- \frac{4\gamma}{\gamma+1}\frac{Kn}{\mathrm{Pr}}(1-r^*)\end{aligned} \tag{23}$$

In fully developed flow, it is usual to utilize the mean fluid temperature, T_m, rather than the center line temperature when defining the Nusselt number. This mean or bulk temperature is given by

$$T_m = \frac{\int \rho u T \mathrm{d}A}{\int \rho u \mathrm{d}A} \tag{24}$$

The forced convective heat transfer coefficient is given as follows:

$$h = \frac{q_w}{T_w - T_m} \tag{25}$$

Table 1
Nusselt number values for different values of r^* at $Kn = 0.0$

r^*	Case A		Case B	
	Present	Ref. [20]	Present	Ref. [20]
0	4.36364	4.36364	∞	∞
0.2	4.88259	4.88259	8.49892	8.49892
0.4	4.97917	4.97917	6.58330	6.58330
0.6	5.09922	5.09922	5.91171	5.91171
0.8	5.23654	5.23654	5.57849	5.57849
1.0	5.38462	5.38462	5.38462	5.38462

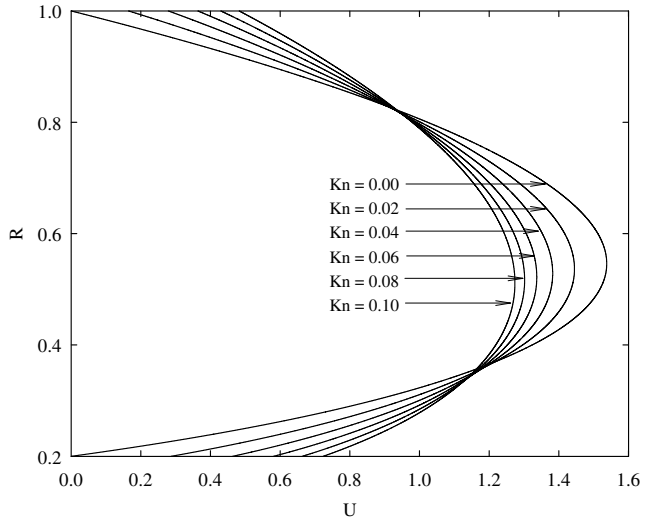

Fig. 2. Dimensionless velocity distributions at different values of Kn.

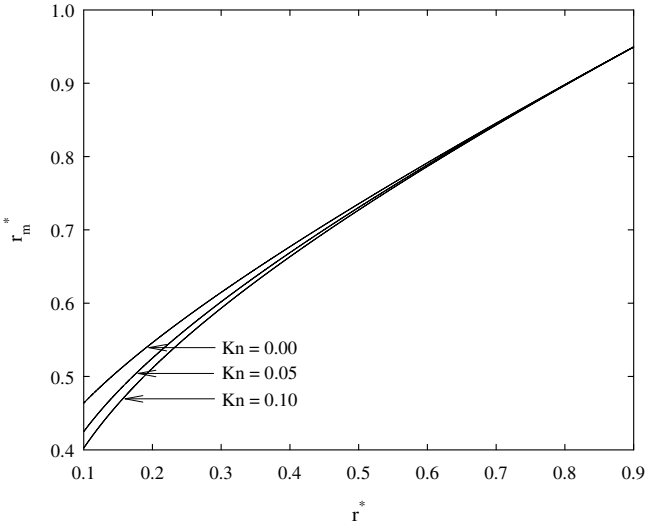

Fig. 3. The variation of r_m^* at different values of Knudsen number.

which is obtained from Nusselt number that is defined as

$$Nu = \frac{q_w D_h}{(T_w - T_m)k} = -\frac{2}{\theta_m^*}(1 - r^*) \tag{26}$$

3. Results and discussion

The forced convection flow in the concentric cylindrical annular microduct is studied. The problem is steady, laminar, and hydrodynamically and thermally fully developed. Two different cases of the thermal boundary conditions are considered: uniform heat flux at the outer wall and adiabatic inner wall (Case A) and uniform heat flux at the inner wall and adiabatic outer wall (Case B). These two cases have been studied for different values of the aspect ratio, r^*, the Knudsen number, Kn and the Brinkman number, Br.

In order to validate the results, they are compared with those of Ref. [20] for the case without the viscous dissipation ($Br = 0$) and the microscale effects ($Kn = 0$). As seen from Table 1, an excellent agreement is obtained.

Fig. 2 illustrates the nondimensional velocity profiles obtained from Eq. (6) for different values of the Knudsen number, Kn at $r^* = 0.2$. The velocity values at $R = 0.2$ and $R = 1$ (which are for the inner and outer walls of the annulus with an aspect ratio of $r^* = 0.2$, respectively) represent the nondimensional values of the velocity slip. As shown, the velocity distribution is not symmetrical, nor are the slip velocities at the walls. A maximum in the velocity occurs close to the inner wall, as expected. Increasing Kn results in an increase in the slip velocities at the inner and outer wall of the micro annulus, while the maximum velocity decreases with the increasing Kn. The variation of the maximum velocity point, r_m^*, with

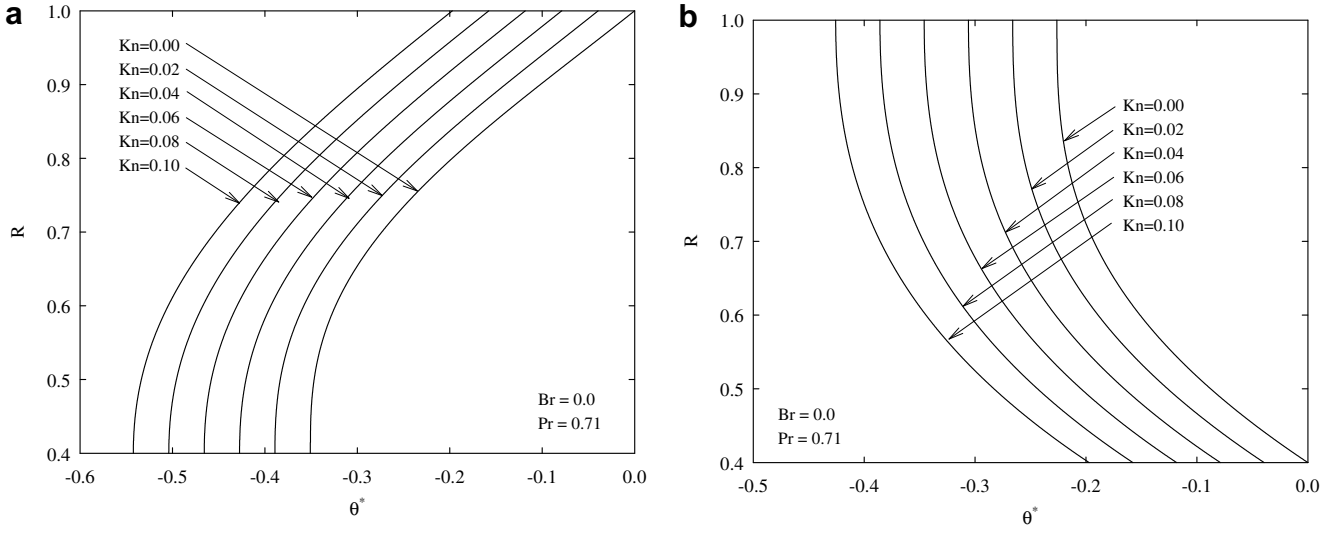

Fig. 4. Dimensionless temperature distributions at different values of Kn for $r^* = 0.4$: (a) Case A and (b) Case B.

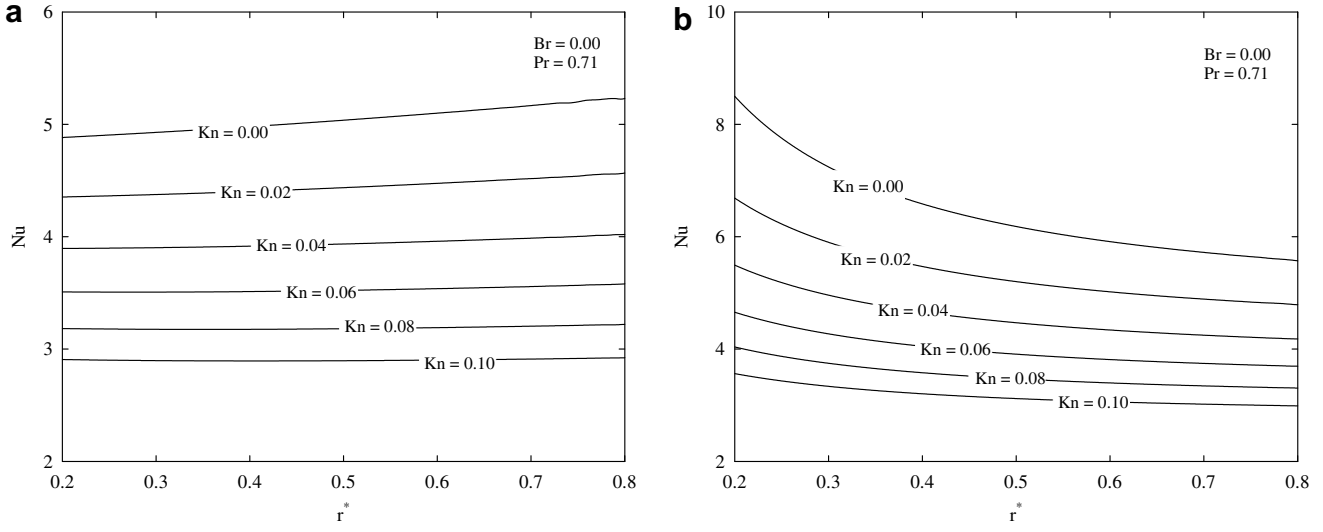

Fig. 5. The variation of Nu with r^* at different values of Kn for $Br = 0.0$: (a) Case A and (b) Case B.

the aspect ratio, r^*, for different values of Kn is seen in Fig. 3. For the values of $r^* < 0.5, r^*_m$ decreases with an increase in Kn, which means that the maximum dimensionless velocity occurs at a closer point to the inner wall.

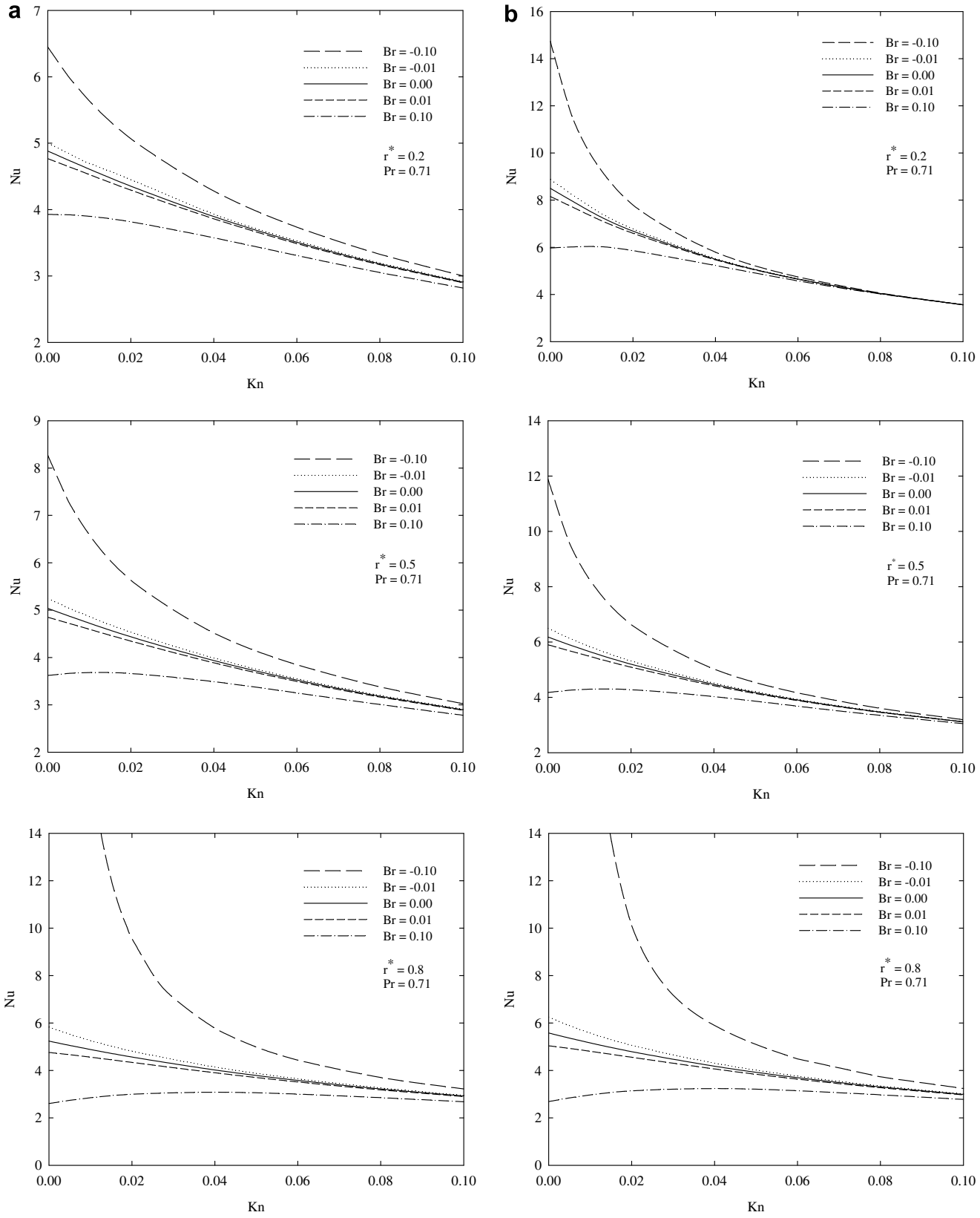

Fig. 6. The variation of Nu with Kn at different values of Br for $r^* = 0.2$, 0.5 and 0.8: (a) Case A and (b) Case B.

For the values of $r^* > 0.5$, Kn has negligible effect on r^*_m, which means the point of the maximum dimensional velocity stays nearly the same.

Fig. 4a and b shows the nondimensional temperature profiles from Eqs. (22) and (23) for various Kn at $r^* = 0.4$ for the Cases A and B, respectively. The temperature values at $R = 0.4$ and $R = 1$ (which are for the inner and outer walls of the annulus with an aspect ratio of $r^* = 0.4$, respectively) represent the nondimensional values of the temperature jump. An increase in Kn results in decreasing nondimensional temperature profile.

From the engineering point of view, the heat transfer rates are important, and can be predicted from the Nusselt number. Fig. 5a and b illustrates the variation of the Nusselt number with the aspect ratio of the annulus, r^* for different values of the Knudsen number at Cases A and B without viscous dissipation ($Br = 0$), respectively. For the both cases, the influence of the increasing Kn is to decrease the heat transfer rates. As expected, for the Case A, an increase in r^* increases Nu, while it decreases Nu for the Case B. However, this Nu-dependence on r^* becomes negligible with increasing Kn.

The variation of the Nusselt number with the Knudsen number for different values of the Brinkman number and the aspect ratio of the annulus, r^* at Cases A and B, respectively, is shown in Fig. 6. An increase at Kn decreases the Nu due to the temperature jump at the wall. Nu decreases with increasing Br for the hot wall (i.e. the wall heating case). For this case, the wall temperature is greater than that of the bulk fluid. Viscous dissipation increases the bulk fluid temperature especially near the wall since the highest shear rate occurs in this region. Hence, it decreases the

Table 2
Nusselt number values for different values of r^* with Kn and Br (Case A)

Kn							
r^*	Br	0.00	0.02	0.04	0.06	0.08	0.10
0.2	−0.10	6.4516	5.0669	4.2784	3.7348	3.3255	3.0016
	−0.01	5.0043	4.4518	3.9302	3.5296	3.1962	2.9159
	0.00	4.8826	4.3530	3.8950	3.5082	3.1824	2.9067
	0.01	4.7667	4.2925	3.8604	3.4870	3.1688	2.8975
	0.10	3.9274	3.8154	3.5746	3.3075	3.0512	2.8176
0.5	−0.10	8.2731	5.6285	4.5136	3.8444	3.3766	3.0224
	−0.01	5.2416	4.5321	3.9859	3.5518	3.1994	2.9081
	0.00	5.0365	4.4361	3.9348	3.5221	3.1808	2.8960
	0.01	4.8469	4.3441	3.8850	3.4928	3.1625	2.8839
	0.10	3.6202	3.6606	3.4876	3.2496	3.0065	2.7797
0.8	−0.10	−491.839	9.5661	5.7775	4.4318	3.6984	3.2163
	−0.01	5.8253	4.8150	4.1441	3.6480	3.2610	2.9491
	0.00	5.2365	4.5663	4.0197	3.5800	3.2196	2.9226
	0.01	4.7559	4.3364	3.8991	3.5100	3.1775	2.8957
	0.10	2.6044	2.9962	3.0799	2.9996	2.8493	2.6773

Table 3
Nusselt number values for different values of r^* with Kn and Br (Case B)

Kn							
r^*	Br	0.00	0.02	0.04	0.06	0.08	0.10
0.2	−0.10	14.7379	7.7895	5.7899	4.7393	4.0540	3.5576
	−0.01	8.8746	6.7831	5.5218	4.6637	4.0386	3.5620
	0.00	8.4989	6.6870	5.4935	4.6554	4.0369	3.5625
	0.01	8.1538	6.5937	5.4656	4.6472	4.0352	3.5630
	0.10	5.9712	5.8580	5.2260	4.5744	4.0199	3.5675
0.5	−0.10	11.8893	6.6322	5.0209	4.1642	3.6017	3.1913
	−0.01	6.4927	5.3149	4.5178	3.9328	3.4829	3.1255
	0.00	6.1810	5.2001	4.4680	3.9087	3.4702	3.1183
	0.01	5.8979	5.0902	4.4194	3.8848	3.4575	3.1112
	0.10	4.1760	4.2767	4.0248	3.6827	3.3479	3.0486
0.8	−0.10	−72.7854	10.1193	5.8938	4.4815	3.7280	3.2376
	−0.01	6.2516	5.0586	4.3034	3.7599	3.3435	3.0120
	0.00	5.5785	4.7881	4.1783	3.6945	3.3054	2.9889
	0.01	5.0363	4.5527	4.0599	3.6301	3.2686	2.9660
	0.10	2.6863	3.1396	3.2360	3.1417	2.9692	2.7755

temperature difference between the wall and the bulk fluid, which is the main driving mechanism for the heat transfer from wall to fluid. However, for the cold wall (i.e. the wall cooling case), the viscous dissipation increases the temperature differences between the wall and the bulk fluid by increasing the fluid temperature more. Therefore, increasing *Br* in the negative direction increases *Nu*. As seen from the figure, the behavior of *Nu* versus *Kn* for lower values of the Brinkman number, either in the case of wall heating ($Br = 0.01$) or in the case of the wall cooling ($Br = -0.01$) is very similar to that of $\mathrm{Br} = 0$. In addition, as observed from the figure, *Br* is more effective on *Nu* for lower values of *Kn* than for higher values of *Kn*.

Tables 2 and 3 summarize some typical results of this study.

4. Conclusions

In this study, we have obtained analytical solutions for hydrodynamically and thermally fully developed, laminar, steady, convective heat transfer problem in concentric annular micro ducts. The analysis includes the influence of the viscous dissipation and the aspect ratio of the annulus, r^* in addition to the slip velocity and temperature jump prescriptions at the wall. The interactive effects of the Brinkman number and Knudsen number on the Nusselt number have been studied. Two different orientations of the wall thermal boundary conditions have been considered, namely: uniform heat flux at the outer wall and adiabatic inner wall (Case A) and uniform heat flux at the inner wall and adiabatic outer wall (Case B). The expressions for the Nusselt number in terms of the aspect ratio of the annulus, r^*, the Knudsen, *Kn* and the Brinkman number, *Br* have been obtained.

Acknowledgement

The authors greatly acknowledge the financial support of this work by the Scientific and Technological Research Council of Turkey (TUBITAK) under Grant No. 104M436.

References

[1] C.M. Ho, C.Y. Tai, Micro-electro-mechanical systems (MEMS) and fluid flows, Annu. Rev. Fluid Mech. 30 (1998) 579–612.
[2] B. Palm, Heat transfer in microchannels, Microscale Thermophys. Eng. (2001) 155–175.
[3] C.B. Sobhan, S.V. Garimella, A comparative analysis of studies on heat transfer and fluid flow in microchannels, Microscale Thermophys. Eng. 5 (2001) 293–311.
[4] N.T. Obot, Toward a better understanding of friction and heat/mass transfer in microchannels – a literature review, Microscale Thermophys. Eng. 6 (2002) 155–173.
[5] A.A. Rostami, N. Saniei, A.S. Mujumdar, Liquid flow and heat transfer in microchannels: a review, Heat Technol. 18 (2000) 59–68.
[6] A.A. Rostami, A.S. Mujumdar, N. Saniei, Flow and heat transfer for gas flowing in microchannels: a review, Heat Mass Transfer 38 (2002) 359–367.
[7] M. Gad-el-Hak, Flow physics in MEMS, Mec. Ind. 2 (2001) 313–341.
[8] Z.Y. Guo, Z.X. Li, Size effect on microscale single-phase flow and heat transfer, Int. J. Heat Mass Transfer 46 (2003) 59–149.
[9] Z.Y. Guo, Z.X. Li, Size effect on single-phase channel flow and heat transfer at microscale, Int. J. Heat Fluid Flow 24 (3) (2003) 284–298.
[10] G.L. Morini, Single-phase convective heat transfer in microchannels: a review of experimental results, Int. J. Therm. Sci. 43 (2004) 631–651.
[11] R.F. Barron, X.M. Wang, R.O. Warrington, T.A. Ameel, Evaluation of the eigenvalues for the Graetz problem in slip-flow, Int. Commun. Heat Mass Transfer 23 (4) (1996) 563–574.
[12] R.F. Barron, X. Wang, T.A. Ameel, R.O. Warrington, The Graetz problem extended to slip-flow, Int. J. Heat Mass Transfer 40 (8) (1997) 1817–1823.
[13] T.A. Ameel, X.M. Wang, R.F. Baron, R.O. Warrington, Laminar forced convection in a circular tube with constant heat flux and slip flow, Microscale Thermophys. Eng. 1 (4) (1997) 303–320.
[14] O. Aydın, M. Avcı, Heat and flow characteristics of gases in micropipes, Int. J. Heat Mass Transfer 49 (2006) 1723–1730.
[15] O. Aydın, M. Avcı, Analysis of laminar heat transfer in micro-Poiseuille Flow, Int. J. Therm. Sci. 46 (2007) 30–37.
[16] O. Aydın, M. Avcı, Analysis of micro-Graetz problem in a microtube, Nanoscale Microscale Thermophys. Eng. 10 (2006) 345–358.
[17] O. Aydın, M. Avcı, Thermally developing flow in microchannels, J. Thermophys. Heat Transfer 20 (3) (2006) 628–631.
[18] T.M. Adams, S.I. Abdel-Khalik, S.M. Jeter, Z.H. Qureshi, An experimental investigation of single-phase forced convection in microchannels, Int. J. Heat Mass Transfer 41 (1998) 851–857.
[19] G. Kardinakis, A. Beskok, N. Aluru, Microflows and Nanoflows: Fundamentals and Simulation, Springer Science + Business Media, New York, 2005, pp. 61–64.
[20] M. Avcı, O. Aydın, Laminar forced convection with viscous dissipation in a concentric annular duct, Comptes Rendus Mec. 334 (2006) 164–169.